Jarzynski equality in van der Pol and Rayleigh oscillators

Hideo Hasegawa*

Department of Physics, Tokyo Gakugei University, Koganei, Tokyo 184-8501, Japan

(Received 25 July 2011; revised manuscript received 7 November 2011; published 7 December 2011)

We have studied the Jarzynski equality (JE) in van der Pol and Rayleigh oscillators, which are typical deterministic non-Hamiltonian models but not expected to rigorously satisfy the JE because they are not reversible. Our simulations that calculate the contribution to the work W of an applied ramp force with a duration τ show that the JE approximately holds for a fairly wide range of τ including $\tau \to 0$ and $\tau \to \infty$, except for $\tau \sim T$, where T denotes the period of relaxation oscillations in the limit cycle. The work distribution function (WDF) is shown to be non-Gaussian with the U-shaped structure for a strong damping parameter. The τ dependence of R $(=-k_BT\ln\langle e^{-\beta W}\rangle)$ obtained by our simulations is semiquantitatively elucidated with the use of a simple expression for limit-cycle oscillations, where the bracket $\langle\cdot\rangle$ expresses an average over the WDF. The result obtained in self-excited oscillators is in contrast with the fact that the JE holds in the Nosé-Hoover oscillator, which also belongs to deterministic non-Hamiltonian models.

DOI: 10.1103/PhysRevE.84.061112 PACS number(s): 05.70.−a, 05.45.−a, 05.40.−a

I. INTRODUCTION

In the last decade, a significant progress has been made in theoretical studies on nonequilibrium statistics (for reviews, see Refs. [1–3]). The important three fluctuation theorems have been proposed: the Jarzynski equality (JE) [4], the steady-state and transient fluctuation theorems [5–8], and the Crooks theorem [7,8]. They may be applicable to nonequilibrium systems driven arbitrarily far from the equilibrium states. In this paper we pay our attention to the JE expressed by

$$\langle e^{-\beta W}\rangle = \int dW\ P(W)\, e^{-\beta W} = e^{-\beta \Delta F}, \tag{1}$$

where W denotes a work made in a system when its parameter is changed, the bracket $\langle\cdot\rangle$ expresses the average over the work distribution function (WDF), $P(W)$, of a work performed by a prescribed protocol, ΔF stands for the free-energy difference between the initial and final equilibrium states, and β $(=1/k_BT)$ is the inverse temperature of the initial state. Equation (1) includes the second law of thermodynamics, $\langle W\rangle \geqslant \Delta F$, where the equality holds only for the reversible process. The JE was originally proposed for a classical isolated system and open system weakly coupled to baths that are described by the Hamiltonian [4] and the stochastic models [9]. Jarzynski later proved that the JE is valid for strongly coupled open systems [10]. The validity of the JE has been confirmed by some experiments for systems that can be described by damped harmonic oscillator models [11–16]. Stimulated by these experiments, many theoretical analyses have been made for harmonic oscillators with the use of the Markovian Langevin model [13–16], the non-Markovian Langevin model [17–20], Fokker-Planck equation [21], and Hamiltonian model [22–27]. Recently the validity of the JE in nonlinear oscillators with anharmonic potentials has been investigated in Refs. [18,28].

In this paper we study the self-excited oscillators described by van der Pol and Rayleigh equations with state- and velocity-dependent dampings [29,30]. They are expressed by

$$\dot{x} = v, \tag{2}$$

$$\dot{v} = -x - \zeta\, v + f(t), \tag{3}$$

$$\zeta = \begin{cases} c(x^2 - a) & \text{for the van der Pol model,} \\ c(v^2 - a) & \text{for the Rayleigh model,} \end{cases} \tag{4}$$

where $v = \dot{x}$, $a = 1$, c $(\geqslant 0)$ is a damping parameter, the dot $(\cdot)$ denotes a derivative with respect to time t, ζ stands for an auxiliary variable, and $f(t)$ expresses an applied external force. Conditions of $\zeta > 0$ and $\zeta < 0$ express positive and negative dissipations, respectively. The van der Pol equation was proposed as a mathematical model of self-excited oscillations for a simple electric circuit with nonlinear triode valve [29]. The Rayleigh equation was introduced to show the appearance of sustained vibrations in acoustics [30]. Van der Pol and Rayleigh equations are formally equivalent in the sense that the van der Pol equation can be transformed to the Rayleigh equation and vice versa with a proper change of variables. These equations provide basic models for various nonlinear dynamics of systems in mechanical and electrical engineering, biology, biochemistry, and many other applications (for a recent review of nonlinear equations, see Ref. [31]). Many studies have been reported of the van der Pol model, which can be regarded as a special case of the FitzHugh-Nagumo model [32,33]. The properties of periodic solutions of the van der Pol oscillator are known in considerable detail for a sufficiently small or large damping coefficient.

The van der Pol and Rayleigh oscillators belong to deterministic non-Hamiltonian models. The Nosé-Hoover (NH) oscillator [34,35], which has been widely adopted for a study of molecular dynamics, also belongs to non-Hamiltonian models. The NH oscillator is described by [34,35]

$$\dot{x} = v, \tag{5}$$

$$\dot{v} = -x - \zeta\, v + f(t), \tag{6}$$

$$\dot{\zeta} = \frac{1}{\tau_Q}(v^2 - k_BT), \tag{7}$$

*hideohasegawa@goo.jp

 ©2011 American Physical Society

where ζ is a state variable of the thermal reservoir with the temperature T and τ_Q stands for the relaxation time of ζ. It is noted that Eqs. (2)–(4) with $a = k_B T$ are similar to Eqs. (5)–(7) except for the fact that Eq. (4) is given by ζ while Eq. (7) is expressed by $\dot{\zeta}$ [36,37]. The fluctuation theorem in a non-Hamiltonian system coupled to a thermostat has been discussed in Refs. [5,6,38–40]. References [41–43] have provided the condition for the JE to hold in a non-Hamiltonian (and Hamiltonian) model. The condition requires that the equilibrium canonical distribution should be given by [43]

$$P(\boldsymbol{Q},\boldsymbol{q},\lambda) \propto e^{-\beta H(\boldsymbol{Q},\lambda)}\, e^{-\beta\psi(\boldsymbol{q})}, \tag{8}$$

with

$$\psi(\boldsymbol{q}) = -k_B T \ln \phi(\boldsymbol{q}), \tag{9}$$

where $H(\boldsymbol{Q})$ denotes energy of the system, $\phi(\boldsymbol{q})$ is the (normalized) equilibrium distribution of bath variable $\boldsymbol{q}$, and λ is an external parameter. The canonical distribution of the Nosé-Hoover model with $f(t) = \lambda$ is given by [35]

$$P(x,v,\zeta) \propto e^{-\beta(x^2/2-\lambda x+v^2/2+\tau_Q\zeta^2/2)}, \tag{10}$$

which satisfies the condition given by Eqs. (8) and (9) with $\boldsymbol{Q} = (x,v)$ and $\boldsymbol{q} = \zeta$, and then the JE holds in the Nosé-Hoover model [41–43]. In contrast, the equilibrium distribution of the van der Pol or Rayleigh oscillator, which is an odd-shaped racetrack [44], does not meet the condition given by Eqs. (8) and (9). Although this suggests that the JE does not hold in van der Pol and Rayleigh oscillators, it is worthwhile to examine how and to what extent the JE is violated in self-excited oscillators, which is the purpose of the present paper.

The paper is organized as follows. In the next section, Sec. II, we briefly explain basic equations of van der Pol and Rayleigh oscillators. We examine the validity of the JE by simulations applying a ramp force with a duration τ. Our simulations in Sec. III show that although the JE is not exactly satisfied in self-excited oscillators, it approximately holds in a fairly wide range of τ values including $\tau \to 0$ (transient force) and $\tau \to \infty$ (quasistationary force). Various types of analytical solutions for applied sinusoidal forces have been developed for van der Pol and Rayleigh models. It is, however, still difficult to obtain analytical solutions for arbitrary external forces including nonperiodic ones. By using a simple analytic expression of solutions for an applied ramp force, which is suggested by He's method for a limit cycle of self-excited oscillators [45], we present in Sec. IV a semiquantitative analysis of the results of our simulations. Section V is devoted to our conclusion.

II. SELF-EXCITED OSCILLATOR MODELS

A. Energy, heat, and work

From Eqs. (2)–(4), van der Pol and Rayleigh oscillators are described by

$$\ddot{x} + x + \zeta\, v = f(t), \tag{11}$$

with

$$\zeta = \begin{cases} c(x^2-1) & \text{for the van der Pol model,} \\ c(v^2-1) & \text{for the Rayleigh model.} \end{cases} \tag{12}$$

When we set $\zeta = c$ (>0) in Eq. (11), it expresses a damped harmonic oscillator. Multiplying $\dot{x}$ for the both sides of Eq. (11) and integrating them over t, we obtain

$$U(t) - U(0) = Q(t) + W_c(t), \tag{13}$$

with

$$U(t) = \frac{\dot{x}(t)^2}{2} + \frac{x(t)^2}{2}, \tag{14}$$

$$Q(t) = -\int_0^t \zeta\, \dot{x}^2\, dt, \tag{15}$$

$$W_c(t) = \int_0^t f(t)\, \dot{x}\, dt, \tag{16}$$

where $U(t)$, $Q(t)$, and $W_c(t)$ stand for the internal energy, heat (dissipative energy), and classical work, respectively. Equation (13) expresses the first law of thermodynamics. In order to show the JE, Jarzynski employed an alternative work defined by [4]

$$W_J(t) = -\int_0^t \dot{f}(t)\, x(t)\, dt, \tag{17}$$

which is related with $W_c(t)$ as

$$W_J(t) = -f(t)x(t) + f(0)x(0) + W_c(t). \tag{18}$$

It is noted that $U(t)$, $Q(t)$, $W_c(t)$, and $W_J(t)$ depend on a microscopic history of the system of $x(t)$ and $v(t)$ for $t \geqslant 0$ starting from their initial values of $x(0)$ ($=x_0$) and $v(0)$ ($=v_0$). $W_J(t)$ has been employed for a study of the JE in this study.

We have presented in the Appendix some numerical calculations of thermodynamical quantities such as energy, heat, and work of the van der Pol oscillator, which are evaluated both by single and multiple runs of simulations. It should be note that even for $f(t) = 0$, we obtain $\langle U(t)\rangle_0 - \langle U(0)\rangle_0 \neq 0$ in van der Pol (and Rayleigh) oscillators because of a dissipative contribution of $\langle dQ(t)/dt\rangle_0$ (see Figs. 12 and 13 in the Appendix), where $\langle\cdot\rangle_0$ stands for an average over initial states Eqs. (22) and (23). This is in contrast to the NH oscillator where the relations $\langle U(t)\rangle_0 - \langle U(0)\rangle_0 = 0$ and $\langle dQ(t)/dt\rangle_0 = 0$ hold. This difference reflects on the difference in nonequilibrium properties of self-excited and NH oscillators: The JE does not hold in the former, while it holds in the latter.

B. The Jarzynski equality

For a study of the JE, we will apply a ramp force $f(t)$ given by

$$f(t) = \begin{cases} 0 & \text{for} \quad t < 0, \\ g\left(\frac{t}{\tau}\right) & \text{for} \quad 0 \leqslant t < \tau, \\ g & \text{for} \quad t \geqslant \tau, \end{cases} \tag{19}$$

where τ denotes a duration of the force and g its magnitude. By using Eqs. (17) and (19), we obtain a work induced by the applied ramp force,

$$W_0 \equiv W_J(\tau) = -\left(\frac{g}{\tau}\right)\int_0^\tau x(t)\,dt. \tag{20}$$

The WDF is expressed by

$$P(W) = \langle \delta(W - W_0)\rangle_0, \tag{21}$$

where $\langle\cdot\rangle_0$ signifies the average over the canonically distributed $\{x_0\}$ and $\{v_0\}$,

$$P(x_0, v_0) \propto e^{-\beta(x_0^2/2 + v_0^2/2)}, \tag{22}$$

satisfying the equipartition relation given by

$$\langle x_0^2\rangle_0 = \langle v_0^2\rangle_0 = k_B T. \tag{23}$$

The JE in Eq. (1) can be rewritten as

$$R \equiv -\frac{1}{\beta}\ln\langle e^{-\beta W}\rangle = \Delta F. \tag{24}$$

If the WDF is Gaussian, R is given by

$$R = \mu - \frac{\beta\sigma^2}{2}, \tag{25}$$

with

$$\mu = \langle W\rangle, \tag{26}$$

$$\sigma^2 = \langle (W-\mu)^2\rangle, \tag{27}$$

which stand for mean and variance, respectively, of the WDF. Of course, Eq. (25) is not valid for non-Gaussian WDF.

III. MODEL CALCULATIONS

A. The van der Pol oscillator

Model calculations of the JE for van der Pol and Rayleigh oscillators will be reported in Secs. III A and IIIB, respectively. We have made simulations, solving Eqs. (11) and (12) by using the Runge-Kutta method with a time step of 0.0001 for initial states of $\{x_0\}$ and $\{v_0\}$ given by Eqs. (22) and (23) with $k_B T = 1.0$.

In order to get some insight into the van der Pol oscillator, we first show results without forces [$f(t) = 0.0$]. Time courses of $x(t)$ and $v(t)$ for a damping parameter of $c = 10.0$ calculated by single runs with $x_0 = 1.0$ and $v_0 = 0.0$ are plotted in Figs. 1(a) and 1(b), respectively. Time courses of $x(t)$ exhibit the relaxation oscillation with characteristic sharp periodic jumps. A parametric plot of $x(t)$ versus $v(t)$ in Fig. 1(c) shows the limit cycle. The period of the relaxation oscillation depends on the magnitude of a damping parameter c. The dashed curve of Fig. 1(d) expresses the c dependence of period T for $f(t) = 0.0$, which is increased with increasing c. When a constant force $f = 0.5$ is applied to the oscillator, its oscillation period is further increased, as shown by the solid curve in Fig. 1(d).

Figure 2(a) shows time courses of $x(t)$ when a ramp force with $\tau = 100.0$ is applied to the van der Pol oscillator for $c = 1.0$ with initial conditions of $x_0 = 1.0$ and $v_0 = 0.0$. The period of the oscillation with the applied ramp force with $g = 0.5$ (solid curve) is gradually increased compared

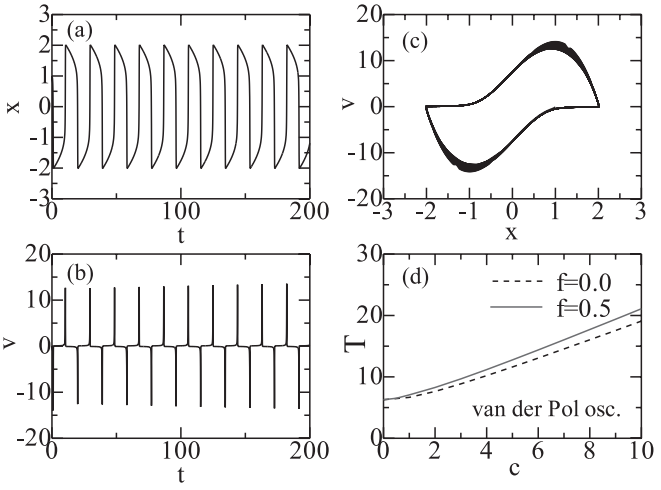

FIG. 1. (Color online) (a) $x(t)$, (b) $v(t)$, and (c) a parametric plot of $x(t)$ vs $v(t)$ in the van der Pol oscillator with $c = 10.0$ for $f(t) = 0.0$ with an initial condition of $x_0 = 1.0$ and $v_0 = 0.0$. (d) The c dependence of a period T with constant forces of $f(t) = 0.0$ (dashed curve) and $f(t) = 0.5$ (solid curve).

to that with $g = 0.0$ (dashed curve). Figure 2(b) shows a similar plot of $x(t)$ for $c = 10.0$. The period of the oscillation with $c = 10.0$ is longer than that with $c = 1.0$ by a factor of about three. An applied ramp force with $g = 0.5$ and $\tau = 100$ induces a work $W_J(t)$ whose time course is shown by the chain (solid) curve for $c = 1.0$ ($c = 10.0$) in Fig. 2(c). We obtain $W_0 = -0.110$ ($W_0 = -0.126$) for $c = 1.0$ ($c = 10.0$) by a single run with initial values of $x_0 = 1.0$ and $v_0 = 0.0$.

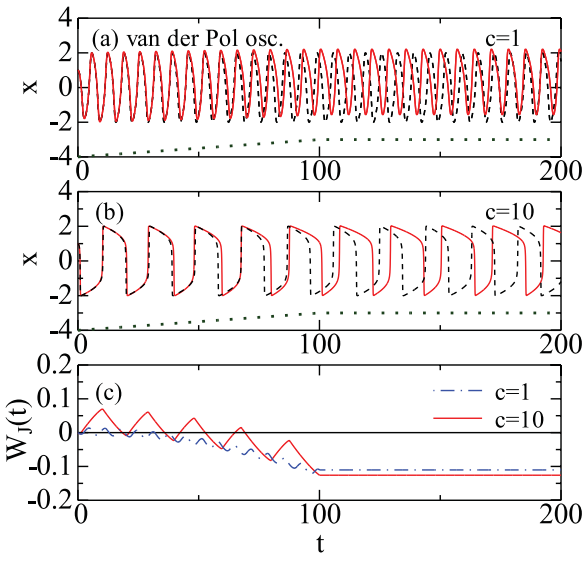

FIG. 2. (Color online) Time courses of $x(t)$ of the van der Pol oscillator with (a) $c = 1.0$ and (b) $c = 10.0$ for ramp forces with $g = 0.0$ (dashed curve) and $g = 0.5$ (solid curve) for $\tau = 100.0$. (c) $W_J(t)$ with $c = 1.0$ (chain curve) and $c = 10.0$ (solid curve) for $g = 0.5$ and $\tau = 100.0$. An applied ramp force $f(t)$ is plotted by dotted curves in (a) and (b). Simulations are performed by single runs with initial conditions of $x_0 = 1.0$ and $v_0 = 0.0$.

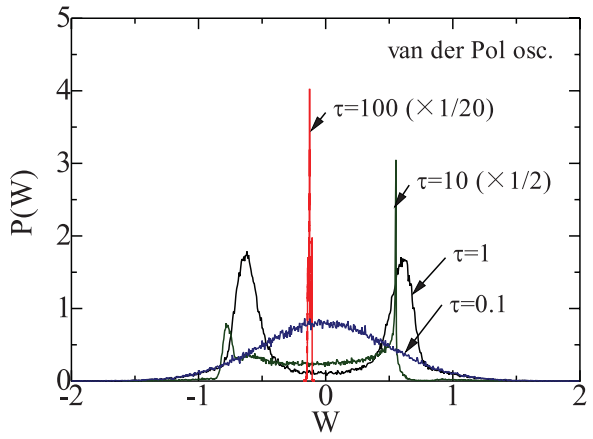

FIG. 3. (Color online) $P(W)$ for $\tau = 0.1$, 1.0, 10.0, and 100.0 with $c = 10.0$ and $g = 0.5$ in the van der Pol oscillator, $P(W)$ for $\tau = 10.0$ and 100.0 being multiplied by factor of 1/2 and 1/20, respectively.

Calculating W_0 in Eq. (20) for given initial states, we have obtained the WDF, $P(W)$, with the use of Eq. (21), whose results for $\tau = 0.1$, 1.0, 10.0, and 100.0 with $c = 10.0$ are plotted in Fig. 3. Although the WDF for $\tau = 0.1$ is Gaussian, those for $\tau = 1.0$, 10.0, and 100.0 are non-Gaussian with the U-shaped structure, which are quite different from the Gaussian distributions obtained in harmonic oscillators. Figure 4 shows $P(W)$ for various values of c with a fixed $\tau = 1.0$. With decreasing the damping parameter from $c = 10.0$, the WDF is changed from the double-peaked distribution to the single-peaked Gaussian-like distribution.

Figures 5(a)–5(c) show τ dependencies of μ, σ, and R, respectively, for $c = 1.0$ (dashed curves), $c = 5.0$ (dotted curves), and $c = 10.0$ (solid curves) for ramp forces with $g = 0.5$. Here μ is almost zero for $\tau = 0.1$, and it gradually decreased to -0.125 for $\tau = 1000.0$. In contrast, $\sigma \simeq 0.5$ at $\tau = 0.1$, and it goes to zero at $\tau = 1000.0$ with a small bump at $\tau \sim 3.0$. The calculated R with $c = 10.0$ (solid curve) is in nearly agreement with ΔF $(=-g^2/2 = -0.125)$ for $\tau \gtrsim 100.0$ and $\tau \lesssim 0.2$, but it significantly deviates from ΔF for $0.2 \lesssim \tau \lesssim 100.0$. The discrepancy of $R \neq \Delta F$ implies a

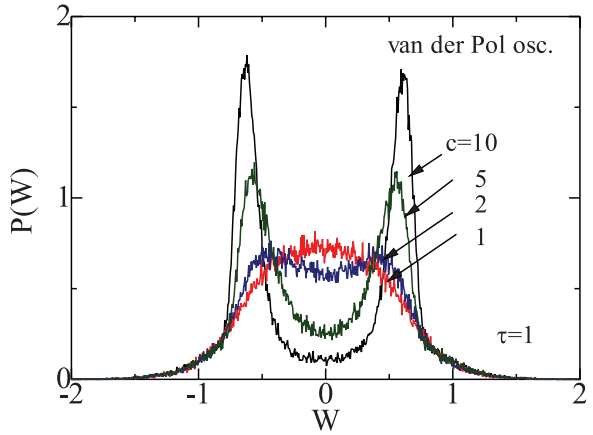

FIG. 4. (Color online) $P(W)$ for $c = 1.0$, 2.0, 5.0, and 10.0 with $\tau = 1.0$ and $g = 0.5$ in the van der Pol oscillator.

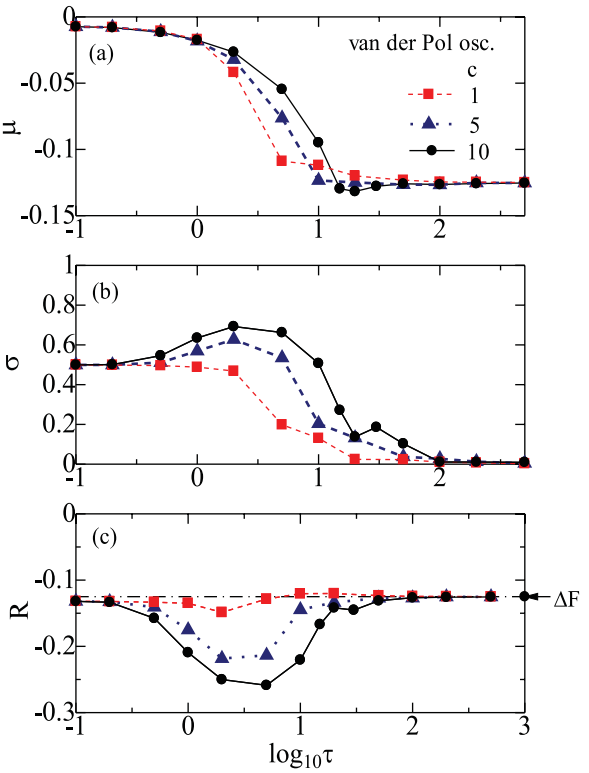

FIG. 5. (Color online) The τ dependence of (a) μ, (b) σ, and (c) R in the van der Pol oscillator with $c = 1.0$ (dashed curve), 5.0 (dotted curve), and 10.0 (solid curve) for ramp forces with $g = 0.5$, the arrow along the right ordinate in (c) expressing ΔF. The JE is expressed by $R = \Delta F$ $(=-0.125)$.

violation of the JE. This deviation becomes less significant for smaller values of $c = 5.0$ and 1.0, and it vanishes for $c = 0.0$ (harmonic oscillator) where the JE holds.

B. The Rayleigh oscillator

Next we study the case of the Rayleigh oscillator. Time courses of $x(t)$ and $v(t)$ of the relaxation oscillation for $c = 10.0$ and $f(t) = 0.0$ are plotted in Figs. 6(a) and 6(b), respectively, and a parametric plot of $x(t)$ versus $v(t)$ in Fig. 6(c) exhibits the limit cycle. The period of the relaxation oscillation depends on the magnitude of c. The dashed curve of Fig. 6(d) expresses the c dependence of the period T for $f(t) = 0.0$, which is increased with increasing c. The period of the oscillator for a constant $f = 0.5$ (solid curve) coincides with that for $f = 0.0$ (dashed curve) in Fig. 6(d).

The dashed (solid) curve in Fig. 7(a) shows $x(t)$ of the Rayleigh oscillator with $c = 1.0$ for ramp forces with $g = 0.0$ $(g = 0.5)$ and $\tau = 100.0$, which is calculated by single runs with initial condition of $x_0 = 1.0$ and $v_0 = 0.0$. We note that $x(t)$ for $g = 0.5$ is gradually shifted upward compared to that for $g = 0.0$. Figure 7(b) shows a similar plot of $x(t)$ for the case of $c = 10.0$, whose period is longer than that for $c = 1.0$ in Fig. 7(a). The time course of $W_J(t)$ for an applied ramp force with $g = 0.5$ and $\tau = 100.0$ is shown by the chain (solid) curve for $c = 1.0$ $(c = 10.0)$ in Fig. 7(c). A work induced by the applied force is $W_0 = -0.123$ $(W_0 = -0.101)$ for $c = 1.0$

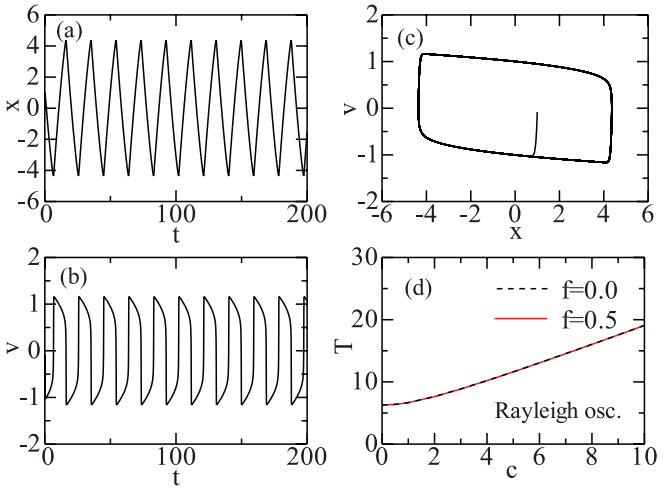

FIG. 6. (Color online) (a) $x(t)$, (b) $v(t)$, and (c) a parametric plot of $x(t)$ vs $v(t)$ in the Rayleigh oscillator with $c = 10.0$ for $f(t) = 0.0$ with the initial condition of $x_0 = 1.0$ and $v_0 = 0.0$. (d) The c dependence of a period T with constant forces of $f(t) = 0.0$ (dashed curve) and $f(t) = 0.5$ (solid curve).

($c = 10.0$) for a given initial condition of $x_0 = 1.0$ and $v_0 = 0.0$.

Calculated WDFs for various τ are plotted in Fig. 8. WDFs for $\tau = 10.0$ and 100.0 have U-shaped structures, while they become the Gaussian-like distribution for $\tau = 0.1$ and 1.0.

Figures 9(a)–9(c) show τ dependencies of μ, σ, and R, respectively, for $c = 1.0$ (dashed curves), $c = 5.0$ (dotted curves), and $c = 10.0$ (solid curves). Their τ dependencies are similar to those for the van der Pol oscillator shown in Figs. 5(a)–5(c). We note that σ for $c = 10.0$ has a large

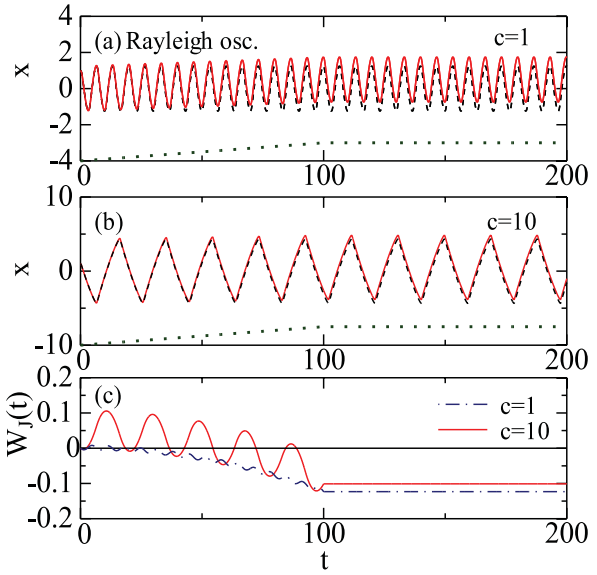

FIG. 7. (Color online) Time courses of $x(t)$ of the Rayleigh oscillator with (a) $c = 1.0$ and (b) $c = 10.0$ for ramp forces with $g = 0.0$ (dashed curve) and $g = 0.5$ (solid curve) for $\tau = 100.0$. (c) $W_J(t)$ with $c = 1.0$ (chain curve) and $c = 10.0$ (solid curve) for $g = 0.5$ with $\tau = 100.0$. An applied ramp force $f(t)$ is plotted by dotted curves in (a) and (b). Simulations are performed by single runs with initial conditions of $x_0 = 1.0$ and $v_0 = 0.0$.

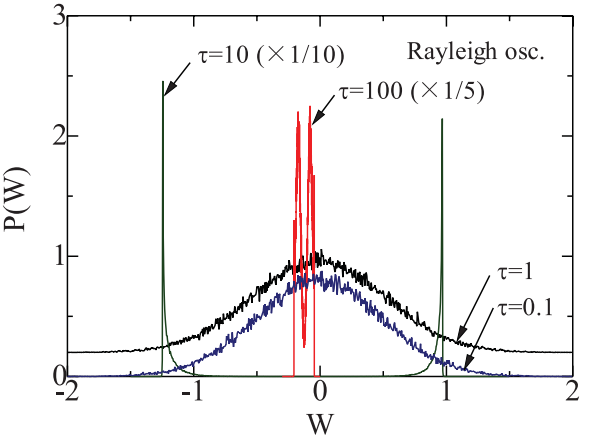

FIG. 8. (Color online) $P(W)$ for $\tau = 0.1$, 1.0, 10.0, and 100.0 with $c = 10.0$ and $g = 0.5$ in the Rayleigh oscillator, $P(W)$ for $\tau = 10.0$ and 100.0 being multiplied by factors of 1/10 and 1/5, respectively, and that for $\tau = 1.0$ being shifted upward by 0.2.

maximum at $\tau \sim 10.0$ where $P(W)$ has the two-peak structure as shown in Fig. 8. The calculated R for $c = 10.0$ (solid curve) is nearly in agreement with ΔF ($=-0.125$) for $\tau \gtrsim 20.0$ and $\tau \lesssim 0.5$, but significantly deviates from ΔF for $0.5 \lesssim \tau \lesssim 20.0$. This deviation is reduced for smaller c values of $c = 5.0$ (dotted curve) and 1.0 (dashed curve), and it vanishes for $c = 0.0$, which corresponds to a harmonic oscillator.

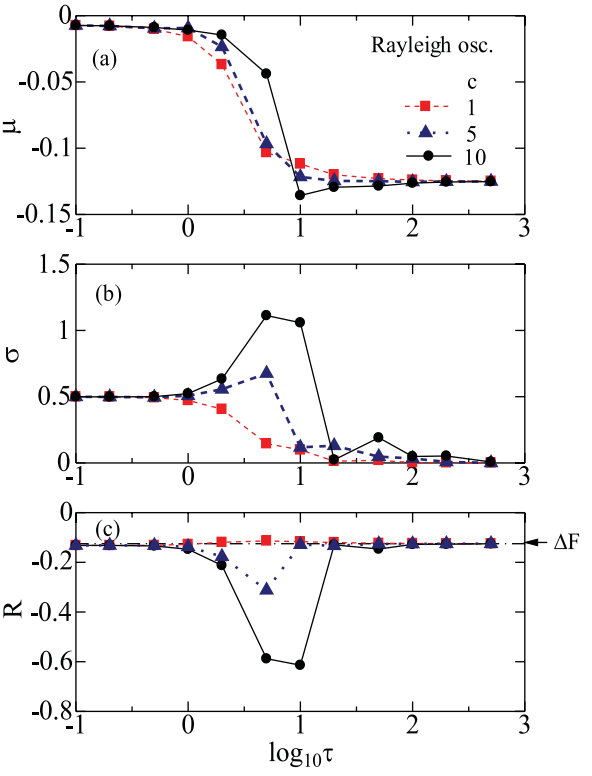

FIG. 9. (Color online) The τ dependence of (a) μ, (b) σ, and (c) R in the Rayleigh oscillator with $c = 1.0$ (dashed curve), 5.0 (dotted curve), and 10.0 (solid curve) for ramp forces with $g = 0.5$, the arrow along the right ordinate in (c) expressing ΔF ($=-0.125$).

IV. DISCUSSION

A. WDF of harmonic oscillators

We have tried to elucidate the result obtained by simulations having been reported in the preceding section. In a recent paper, He [45] has discussed a limit cycle of self-excited oscillators, by using a very simple expression for a relaxation oscillation given by

$$x(t) = A\cos\omega t, \tag{28}$$

where an amplitude A and frequency ω are determined as a function of a damping parameter c with the use of the variational method [45]. It has been shown that they are given by $A = 2.0$ and $\omega = 3.8929/c + O(c^{-2})$ for the van der Pol oscillator with $c \gg 1$ [31,45]. Extending He's method [45], we will study the WDF and the JE of self-excited oscillators in the following.

Before discussing the WDF of self-excited oscillators, we briefly explain that of a harmonic oscillator [$c = 0$ in Eq. (11)],

$$\ddot{x} + x = f(t), \tag{29}$$

whose solution for the applied ramp force $f(t)$ is given by

$$x(t) = x_0\cos t + v_0\sin t + \int_0^t \sin(t-t')f(t')\,dt', \tag{30}$$

$$= x_0\cos t + v_0\sin t + \frac{g(t-\sin t)}{\tau} \quad \text{for} \quad 0 \leqslant t < \tau. \tag{31}$$

From Eq. (20), we obtain a work for a given initial condition of x_0 and v_0,

$$W_0 = Cx_0 + Dv_0 + \phi, \tag{32}$$

with

$$C = -\frac{g\sin\tau}{\tau}, \tag{33}$$

$$D = -\frac{g(1-\cos\tau)}{\tau}, \tag{34}$$

$$\phi = -\frac{g^2}{2} + \frac{g^2(1-\cos\tau)}{\tau^2}. \tag{35}$$

The WDF in Eq. (21) is given by

$$P(W) = \frac{1}{2\pi}\int_{-\infty}^{\infty} e^{iuW}\langle e^{-iuW_0}\rangle_0\,du, \tag{36}$$

with

$$\langle e^{-iuW_0}\rangle_0 \propto \exp(-iu\phi)\int_{-\infty}^{\infty}\exp\left(-\frac{\beta x_0^2}{2} - iuCx_0\right)dx_0 \times \int_{-\infty}^{\infty}\exp\left(-\frac{\beta v_0^2}{2} - iuDv_0\right)dv_0,$$

$$\propto \exp(-iu\phi)\exp\left[-\frac{(C^2+D^2)u^2}{2\beta}\right]. \tag{37}$$

A simple manipulation with Eqs. (36) and (37) leads to the Gaussian WDF given by

$$P(W) = \frac{1}{\sqrt{2\pi\sigma^2}}\,e^{-(W-\mu)^2/2\sigma^2}, \tag{38}$$

with

$$\mu = \phi = -\frac{g^2}{2} + \frac{g^2(1-\cos\tau)}{\tau^2}, \tag{39}$$

$$\sigma^2 = \frac{2g^2(1-\cos\tau)}{\beta\tau^2}. \tag{40}$$

The average of $e^{-\beta W}$ over $P(W)$ in Eq. (1) is given by

$$\langle e^{-\beta W}\rangle = e^{-\beta(\mu-\beta\sigma^2/2)}, \tag{41}$$

which yields

$$R = -\frac{1}{\beta}\ln\langle e^{-\beta W}\rangle, \tag{42}$$

$$= \mu - \frac{\beta\sigma^2}{2} = -\frac{g^2}{2} = \Delta F. \tag{43}$$

Equation (43) implies that the JE holds regardless of a value of τ in harmonic oscillators [13–27].

B. WDF of self-excited oscillators

We now calculate the WDF of self-excited oscillators. Taking into account Eqs. (28) and (31), we have assumed that the solution of the limit cycle in a self-excited oscillator is given by

$$x(t) = A\cos(\omega t - \theta) + \frac{g(t-\sin t)}{\tau} \quad \text{for} \quad 0 \leqslant t < \tau. \tag{44}$$

Here A and ω depend on c as in Ref. [45], and a phase θ is determined by initial conditions of x_0 and v_0,

$$\tan\theta = \frac{v_0}{\omega x_0}, \tag{45}$$

which arises from

$$x_0 = A\cos\theta, \quad v_0 = \omega A\sin\theta. \tag{46}$$

Note that A in a self-excited oscillator is assumed to depend on c but to be independent of initial condition of x_0 and v_0, while A in a harmonic oscillator depends on them as given by $A = \sqrt{x_0^2 + v_0^2}$ in Eq. (31).

Substituting Eq. (44) into Eq. (20), we obtain a work performed by the ramp force for a given θ,

$$W_0 = -\left(\frac{gA}{\omega\tau}\right)[\sin(\omega\tau-\theta) + \sin\theta] - \frac{g^2}{2} + \frac{g^2(1-\cos\tau)}{\tau^2}. \tag{47}$$

The average of $\langle e^{-iuW_0}\rangle_0$ in Eq. (36) is given by

$$\langle e^{-iuW_0}\rangle_0 \propto \int_{-\infty}^{\infty}\int_{-\infty}^{\infty} e^{-\beta x_0^2/2}\,e^{-\beta v_0^2/2}e^{-iuW_0}\,dx_0\,dv_0. \tag{48}$$

Transforming Eq. (48) to the polar coordinate and using Eq. (46), we obtain

$$\langle e^{-iuW_0}\rangle_0 \propto \int_0^{2\pi} e^{-(\beta A^2/2)(\cos^2\theta+\omega^2\sin^2\theta)}\,e^{iu[h(\theta)-\mu]}\,d\theta, \tag{49}$$

with

$$h(\theta) = \left(\frac{gA}{\omega\tau}\right)[\sin(\omega\tau-\theta) + \sin\theta], \tag{50}$$

$$= W_d\,\cos(\theta-\delta), \tag{51}$$

$$W_d = \sqrt{2}\,\sigma = \frac{gA\sqrt{2(1-\cos\omega\tau)}}{\omega\tau}, \tag{52}$$

$$\tan\delta = \frac{(1-\cos\omega\tau)}{\sin\omega\tau}, \tag{53}$$

$$\mu = -\frac{g^2}{2} + \frac{g^2(1-\cos\tau)}{\tau^2}. \tag{54}$$

A substitution of Eq. (49) into Eq. (36) leads to

$$P(W) \propto \int_0^{2\pi} e^{-(\beta A^2/2)(\cos^2\theta+\omega^2\sin^2\theta)}\,\delta[W-\mu+h(\theta)]\,d\theta, \tag{55}$$

which yields the WDF given by

$$P(W) \simeq \left(\frac{1}{\pi}\right)\frac{1}{\sqrt{W_d^2-(W-\mu)^2}} \quad \text{for} \quad -W_d+\mu < W < W_d+\mu. \tag{56}$$

Equation (56) expresses the U-shaped WDF, which is divergent at two edges of $(\pm W_d+\mu)$. Thus when c is increased from zero, the WDF changes from the Gaussian Eq. (38) to U-shaped non-Gaussian Eq. (56), just as shown in Fig. 4.

Figures 10(a) and 10(b) express W_d and μ, respectively, as a function of τ, which are calculated by Eqs. (52) and (54) with $A=2.0$, $g=0.5$, $\omega=2\pi/T$, and $T=19.07$ [Figs. 1(d) and 6(d)]. We note in Fig. 10(a) that the second law of thermodynamics holds because $\mu \geqslant \Delta F$ $(=-0.125)$. W_d has an interesting τ dependence, which is similar to that of σ in harmonic oscillator given by Eq. (40). Two edges of $(\pm W_d+\mu)$ are plotted by solid curves in Fig. 10(c), where squares (circles) express upper and lower edges of the WDF obtained by simulations for the van der Pol oscillator (Rayleigh oscillator). Oscillating behaviors in upper and lower edges of the WDF obtained in simulations are well reproduced in Fig. 10(c).

By using the WDF given by Eq. (56), we can evaluate $\langle e^{-\beta W}\rangle$ in Eq. (1),

$$\langle e^{-\beta W}\rangle = e^{-\beta\mu}\,I_0(\beta W_d), \tag{57}$$

where $I_n(z)$ expresses the modified Bessel function of the first kind. From Eq. (57), R in Eq. (42) is given by

$$R = \mu - \frac{1}{\beta}\ln I_0(\beta W_d). \tag{58}$$

In the limit of $\tau=\infty$, we have $R=\Delta F$ because $\mu=-g^2/2=\Delta F$, $W_d=0.0$, and $I_0(0)=1.0$. In the opposite limit of $\tau=0.0$ where $\mu=0.0$ and $W_d=gA$, we obtain $R=-\beta^{-1}\ln I_0(\beta gA)$, which is generally different from ΔF. By using Eqs. (52), (54), and (58) with $A=2.0$, $g=0.5$, $\omega=2\pi/T$, and $T=19.07$, we have calculated R, which is plotted by the solid curve in Fig. 11. For a comparison, we show by squares and circles results of simulations for van der Pol and Rayleigh oscillators, respectively, with $c=10.0$. We note that the τ dependence of R for $\tau \gtrsim 1.0$ obtained by simulations is semiquantitatively explained by our analysis.

Our calculation, however, yields poor results for $\tau \lesssim 1.0$, where $x(t)$ in Eq. (44) is not a good approximation because an oscillation cannot become a limit cycle for $t \sim \tau \ll T$. Actually with decreasing τ at $\tau \lesssim 1.0$, the WDF is changed from the U-shaped distribution to the Gaussian distribution, as shown in Figs. 3 and 8. Our calculation for $\tau \lesssim 1.0$ can be improved if the WDF is phenomenologically interpolated between the Gaussian and U-shaped distributions as given

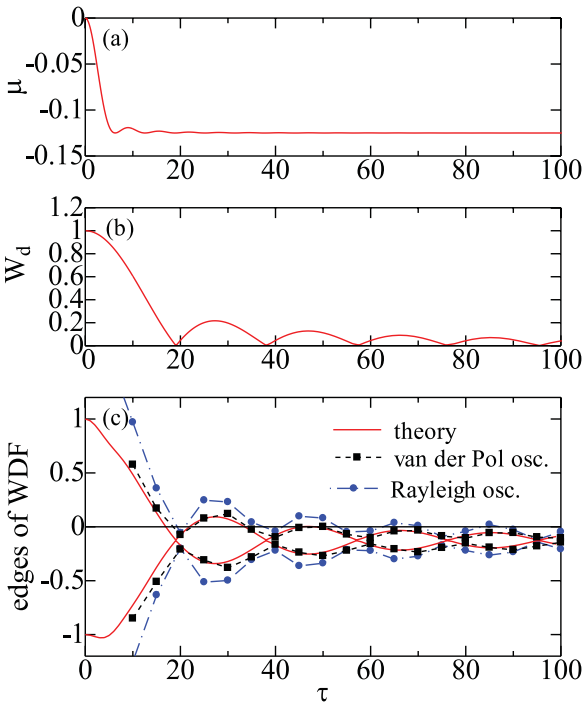

FIG. 10. (Color online) (a) W_d and (b) μ as a function of τ calculated by Eqs. (52) and (54) with $A=2.0$, $g=0.5$, $\omega=2\pi/T$, and $T=19.07$. (c) The τ dependence of $(\pm W_d+\mu)$ (solid curves) and that of upper and lower edges of the WDF obtained by simulations for van der Pol (squares) and Rayleigh oscillators (circles) with $c=10.0$, dashed and chain curves being plotted only for a guide of eye (see text).

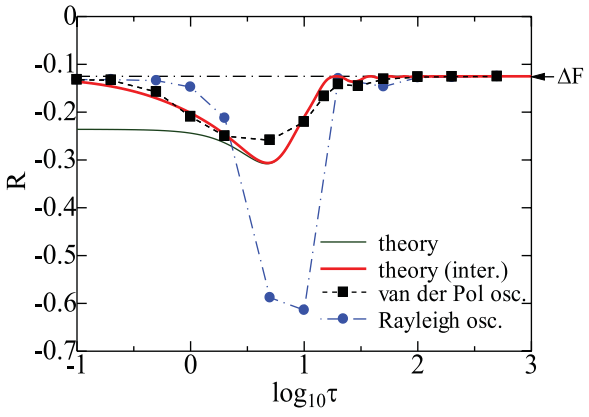

FIG. 11. (Color online) The τ dependence of R calculated by Eq. (58) (solid curves) and Eq. (61) (interpolation: bold solid curve) with $A=2.0$, $g=0.5$, $\omega=2\pi/T$, and $T=19.07$, and those for van der Pol (squares) and Rayleigh oscillators (circles) with $c=10.0$ obtained by simulations, dashed and chain curves being plotted only for a guide of eye. The arrow along the right ordinate expresses ΔF $(=-0.125)$.

by

$$P(W) \propto \frac{p}{\sqrt{2\pi\sigma^2}}\, e^{-(W-\mu)^2/2\sigma^2} + \frac{(1-p)}{\pi}\, \frac{1}{\sqrt{W_d^2 - (W-\mu)^2}}, \tag{59}$$

with

$$p = e^{-\tau/\tau_0}, \tag{60}$$

where τ_0 denotes a parameter. The Gaussian and U-shaped WDFs are dominant for small and large τ, respectively, and they are interpolated between small and large values of τ with a factor p. The average of $\langle e^{-\beta W}\rangle$ is given by

$$\langle e^{-\beta W}\rangle = p\, e^{-\beta(\mu-\beta\sigma^2/2)} + (1-p)\, e^{-\beta\mu} I_0(\beta W_d). \tag{61}$$

The bold solid curve in Fig. 11 expresses R obtained by Eqs. (42), (60), and (61) with $\tau_0 = 1.0$. We note that R deviates from ΔF for $1.0 \lesssim \tau \lesssim 10.0$, although $R \simeq \Delta F$ for $\tau \ll 1.0$ and $\tau \gg 10$, as shown by simulations.

V. CONCLUSION

Studying the JE in van der Pol and Rayleigh oscillators to which a ramp force with a duration τ is applied, we have obtained the following results:

(1) The JE nearly holds in a fairly wide range of τ including transient ($\tau \to 0$) and quasistationary forces ($\tau \to \infty$), although the JE is not rigorously satisfied [41–43],

(2) The WDF has the U-shaped structure for a large damping parameter, and

(3) The τ dependence of R ($=-k_B T \ln\langle e^{-\beta W}\rangle$) [Eq. (24)] obtained by our simulations can be semiquantitatively accounted for by our analysis with a simple expression of $x(t)$ for a limit cycle whose amplitude is assumed to be determined by a damping parameter but not sensitive to initial conditions.

The first item is in contrast with results of NH oscillators where JE holds [41–43]. Derivations of the JE require the condition that the equilibrium canonical distribution of non-Hamiltonian systems satisfies Eqs. (8) and (9) [43]. Van der Pol and Rayleigh oscillators do not meet the condition, while it is held in the NH oscillator [41–43]. Although our simple analysis in item 3 can explain essential features of van der Pol and Rayleigh models, a development of a more advanced theory is desirable for a better understanding of their properties. It would be interesting to examine our result by experiments, for example, by electrical circuits consisting of nonlinear elements.

ACKNOWLEDGMENT

This work is partly supported by a Grant-in-Aid for Scientific Research from Ministry of Education, Culture, Sports, Science and Technology of Japan.

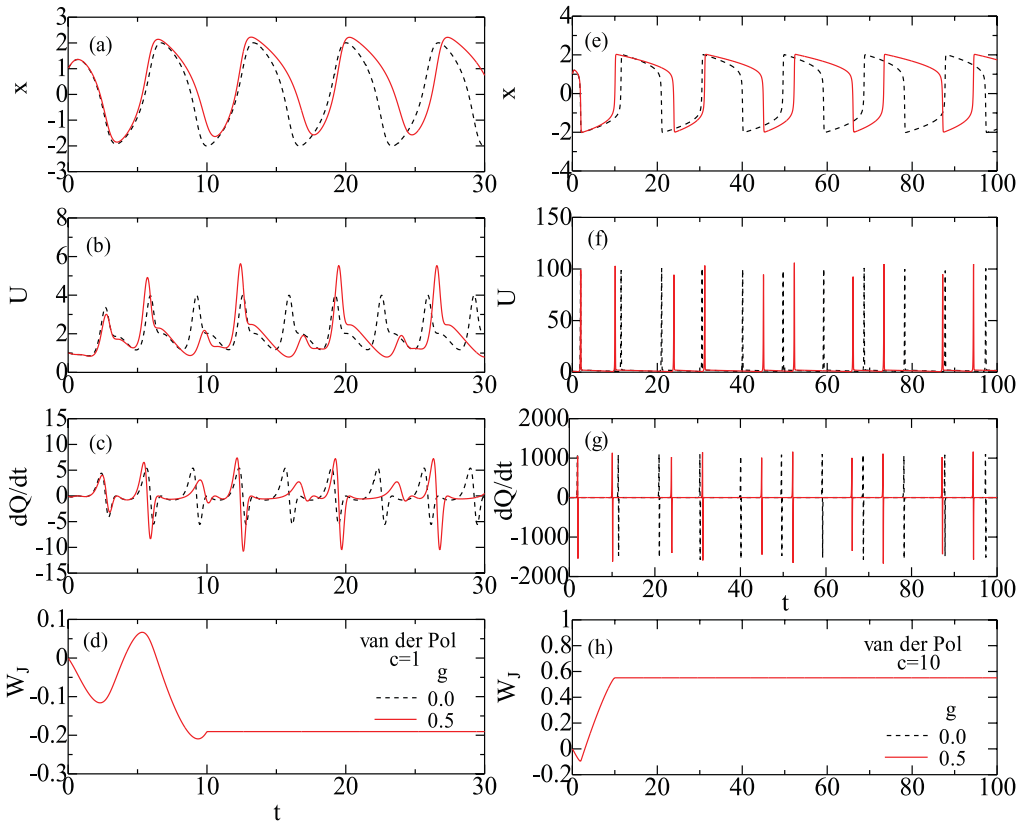

FIG. 12. (Color online) (a) $x(t)$, (b) $U(t)$, (c) $dQ(t)/dt$, and (d) $W_J(t)$ in the van der Pol oscillator with $c = 1.0$, and (e) $x(t)$, (f) $U(t)$, (g) $dQ(t)/dt$, and (h) $W_J(t)$ with $c = 10.0$ for applied ramp forces with $g = 0.0$ (dashed curves) and $g = 0.5$ (solid curves) ($\tau = 10.0$) evaluated by single runs with the initial condition of $x_0 = 1.0$ and $v_0 = 1.0$ yielding $U(0) = 1.0$.

APPENDIX: ENERGY, HEAT, AND WORK OF THE VAN DER POL OSCILLATOR

In this Appendix we will present some model calculations of thermodynamical quantities such as the energy and heat in the van der Pol oscillator, which are evaluated both by single and multiple runs of simulations. Figures 12(a)–12(d) show $x(t)$, $U(t)$, $dQ(t)/dt$, and $W_J(t)$, respectively, of the van der Pol oscillator with $c = 1.0$ for applied ramp forces with $g = 0.0$ (dashed curve) and $g = 0.5$ (solid curve) for $\tau = 10.0$ calculated by single runs with initial conditions of $x_0 = 1.0$ and $v_0 = 1.0$ [$U(0) = 1.0$]. The period of the oscillation with the applied ramp force with $g = 0.5$ is gradually increased compared to that with $g = 0.0$. We obtain $U(t) - U(0) = Q(t)$ for $g = 0.0$ where $W_J(0) = W_c(t) = 0.0$ in Eq. (13). The heat (energy) flows from an environment to the oscillator for $dQ(t)/dt > 0$, and for $dQ(t)/dt < 0$ the heat (energy) flow is reversed. Periodic energy exchanges are realized between the oscillator and environment in the limit cycle. For an applied ramp force with $g = 0.5$, $W_J(t)$ is time dependent at $0 \leqslant t < 10.0$, and it becomes constant ($= -0.191$) at $t \geqslant 10.0$, where $\dot{f}(t) = 0$, as shown in Fig. 12(d).

Figures 12(e)–12(h) show similar plots of relevant thermodynamical quantities in the van der Pol oscillator with a larger damping constant of $c = 10.0$, which are calculated also by single runs with the same initial condition of $x_0 = 1.0$ and $v_0 = 1.0$. The period of relaxation oscillation of $x(t)$ for $c = 10.0$ is larger than that for $c = 1.0$. Time dependencies of $U(t)$ and $dQ(t)/dt$ for $c = 10.0$ become much significant than those for $c = 1.0$: Note that scales of ordinates in Figs. 12(f) and 12(g) are much larger than those in Figs. 12(b) and 12(c). We obtain a positive $W_J(t)$ (=0.551) at $t \geqslant 10.0$ in Fig. 12(h).

Related thermodynamical quantities averaged over 100 000 runs with canonically distributed initial states of $\{x_0\}$ and $\{v_0\}$ with $k_BT = 1.0$ [Eqs. (22) and (23)] are plotted in Fig. 13. Figures 13(a)–13(d) show $\langle x(t)\rangle_0$, $\langle U(t)\rangle_0$, $\langle dQ(t)/dt\rangle_0$, and $\langle W_J(t)\rangle_0$, respectively, of the van der Pol oscillator with $c = 1.0$ for applied forces of $g = 0.0$ (dashed curves) and $g = 0.5$ (solid curves) with $\tau = 10.0$. We note in Fig. 13(a) that although $\langle x\rangle_0 = 0$ for $g = 0.0$, $\langle x\rangle_0$ for $g = 0.5$ at $t \geqslant 10.0$ expresses a small limit-cycle oscillation superposed on a constant of 0.5. This is because random initial states are effectively biased by an applied force. For $g = 0.0$, $\langle U(t)\rangle_0 = 1.0$ at $t = 0.0$, and it becomes about 2.0 at $t \gtrsim 5.0$, which is determined by amplitudes of $x(t)$ and $v(t)$ in the limit cycle, as shown in Fig. 13(b). It is noted that even for $g = 0.0$, we obtain $\langle U(t)\rangle_0 - \langle U(0)\rangle_0 \neq 0.0$, which is due to finite dissipative contributions of $\langle dQ/dt\rangle_0$ ($\neq 0.0$) between an oscillator and environment. Comparing Fig. 13(b) with Fig. 12(b), we note that magnitudes of $\langle U(t)\rangle_0$ become much smaller than those of $U(t)$ for a single run. Owing to an applied ramp force, $\langle U(t)\rangle_0$ for $g = 0.5$ is lower than that for $g = 0.0$. We obtain $\langle W_J\rangle_0 = -0.110$ at $t \geqslant 10.0$ as shown in Fig. 13(d).

Similar plots of relevant thermodynamical quantities for the van der Pol oscillator with a larger $c = 10.0$ are presented in

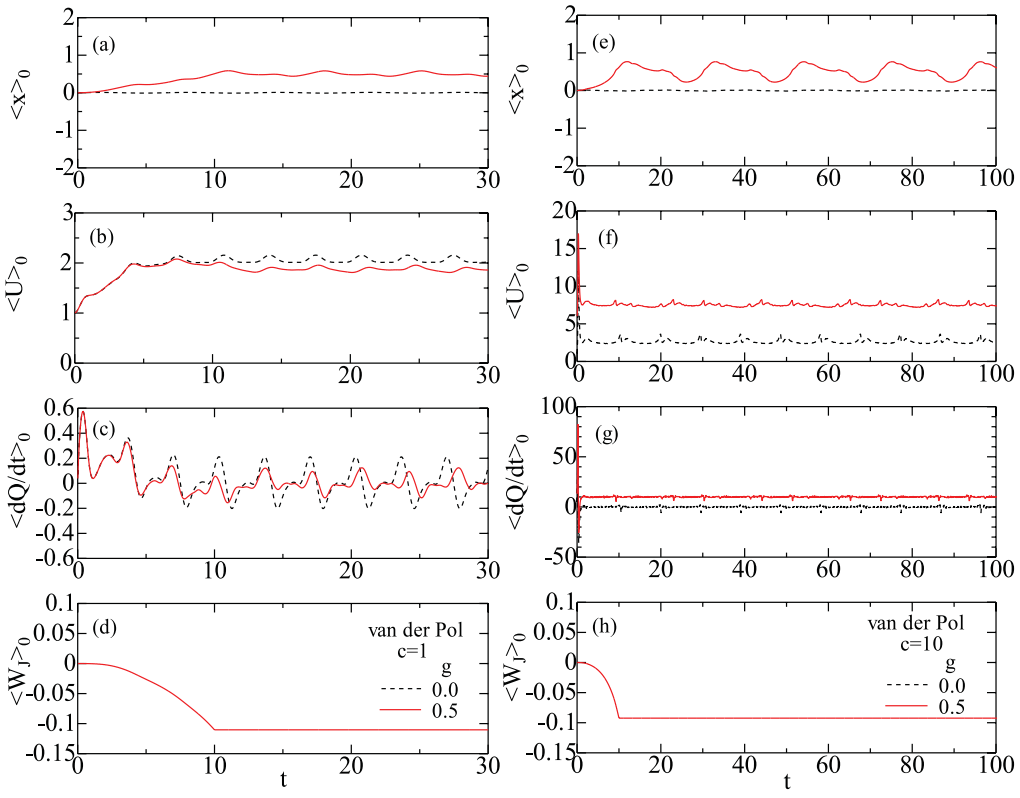

FIG. 13. (Color online) (a) $\langle x(t)\rangle_0$, (b) $\langle U(t)\rangle_0$, (c) $\langle dQ(t)/dt\rangle_0$, and (d) $\langle W_J(t)\rangle_0$ in the van der Pol oscillator with $c = 1.0$, and (e) $\langle U(t)\rangle_0$, (f) $\langle Q(t)\rangle_0$, (g) $\langle dQ(t)/dt\rangle_0$, and (h) $\langle W_J(t)\rangle_0$ with $c = 10.0$ for applied ramp forces with $g = 0.0$ (dashed curves) and $g = 0.5$ (solid curves) ($\tau = 10.0$) averaged over 100 000 runs with $k_BT = 1.0$ ($=\langle U(0)\rangle_0$). Results for $g = 0.5$ in panels (f) and (g) are shifted upward by 5 and 10, respectively, for a clarity of figures.

Figs. 13(e)–13(h). The initial averaged energy of $\langle U(t)\rangle_0 = 1.0$ at $t = 0.0$ is increased to about 2.4–3.6 at $t \gtrsim 5.0$ for $g = 0.0$ in Fig. 13(f). This increase in $\langle U(t)\rangle_0$ is due to energy supplies from environment to the oscillator, which are rapidly accomplished at $0 \leqslant t \lesssim 1.0$ for both $g = 0.0$ and 0.5 as shown in Figs. 13(f) and 13(g). Figure 13(h) shows $\langle W_J\rangle_0 = -0.092$ at $t \geqslant 10.0$, which is in contrast to a positive $W_J = 0.551$ for a single run shown in Fig. 12(h).

[1] C. Bustamante, J. Liphardt, and F. Ritort, Phys. Today **58**, 43 (2005).
[2] F. Ritort, in *Advances in Chemical Physics*, edited by S. A. Rice, Vol. 137 (J. Wiley & Sons, New York, 2008), p. 31.
[3] S. Ciliberto, S. Joubaud, and A. Petrosyan, J. Stat. Mech.: Theor. Exp. (2010) P12003.
[4] C. Jarzynski, Phys. Rev. Lett. **78**, 2690 (1997).
[5] D. J. Evans, E. G. D. Cohen, and G. P. Morriss, Phys. Rev. Lett. **71**, 2401 (1993).
[6] D. J. Evans and D. J. Searles, Phys. Rev. E **50**, 1645 (1994).
[7] O. Narayan and A. Dhar, J. Phys. A **37**, 63 (2004).
[8] G. E. Crooks, Phys. Rev. E **60**, 2721 (1999).
[9] C. Jarzynski, Phys. Rev. E **56**, 5018 (1997).
[10] C. Jarzynski, J. Stat. Mech.: Theor. Exp. (2004) P09005.
[11] J. Liphardt, S. Dumont, S. Smith, I. Tinoco, and C. Bustamante, Science **296**, 1833 (2002).
[12] G. M. Wang, J. C. Reid, D. M. Carberry, D. R. M. Williams, E. M. Sevick, and Denis J. Evans, Phys. Rev. E **71**, 046142 (2005).
[13] F. Douarche, S. Ciliberto, A. Petrosyan, and I. Rabbiossi, Europhys. Lett. **70**, 593 (2005).
[14] F. Douarche, S. Joubaud, N. B. Garnier, A. Petrosyan, and S. Ciliberto, Phys. Rev. Lett. **97**, 140603 (2006).
[15] S. Joubaud, N. B. Garnier, F. Douarche, A. Petrosyan, and S. Ciliberto, Comptes Rendus Phys. **8**, 518 (2007).
[16] S. Joubaud, N. B. Garnier, and S. Ciliberto, J. Stat. Mech.: Theor. Exp. (2007) P09018.
[17] F. Zamponi, F. Bonetto, L. F. Cugliandolo, and J. Kurchan, J. Stat. Mech.: Theor. Exp. (2005) P09013.
[18] T. Mai and A. Dhar, Phys. Rev. E **75**, 061101 (2007).
[19] T. Speck and U. Seifert, J. Stat. Mech.: Theor. Exp. (2007) L09002.
[20] T. Ohkuma and T. Ohta, J. Stat. Mech.: Theor. Exp. (2007) P10010.
[21] S. Chaudhury, D. Chatterjee, and B. J. Cherayil, J. Stat. Mech.: Theor. Exp. (2008) P10006.
[22] A. Dhar, Phys. Rev. E **71**, 036126 (2005).
[23] C. Jarzynski, Comptes Rendus Phys. **8**, 495 (2007).
[24] C. Jarzynski, Eur. Phys. J. B **64**, 331 (2008).
[25] R. Chakrabarti, e-print arXiv:0802.0268.
[26] H. Hijar and J. M. O. de Zárate, Eur. J. Phys. **31**, 1097 (2010).
[27] H. Hasegawa, Phys. Rev. E **84**, 011145 (2011).
[28] A. Saha and J. K. Bhattacharjee, J. Phys. A **40**, 13269 (2007).
[29] B. van der Pol, Philos. Mag. Ser. 7 **2**, 978 (1926); B. van der Pol and J. van der Mark, Nature **120**, 363 (1927).
[30] Lord Rayleigh, Philos. Mag. **15**, 229 (1883).
[31] Ji-Huan He, Int. J. Mod. Phys. B **20**, 1141 (2006).
[32] R. FitzHugh, Biophys. J. **1**, 445 (1961).
[33] J. Nagumo, S. Arimoto, and S. Yoshizawa, Proc. IRE **50**, 2061 (1962).
[34] S. Nosé, Mol. Phys. **52**, 255 (1984); J. Chem. Phys. **81**, 511 (1984).
[35] W. G. Hoover, Phys. Rev. A **31**, 1695 (1985).
[36] Equations (2), (3), and (4b) with $a = k_B T$ correspond to the equations proposed in Ref. [37] for molecular dynamics with coupling to an external bath.
[37] H. J. C. Berendsen, J. P. M. Postma, W. F. van Gunsteren, A. DiNola, and J. R. Haak, J. Chem. Phys. **81**, 3684 (1984).
[38] G. Gallavotti and E. G. D. Cohen, Phys. Rev. Lett. **74**, 2694 (1995).
[39] D. J. Evans and D. J. Searles, Phys. Rev. E **52**, 5839 (1995).
[40] E. M. Sevick, R. Prabhakar, S. R. Williams, and D. J. Searles, Ann. Rev. Phys. Chem. **59**, 602 (2008).
[41] M. A. Cuendet, Phys. Rev. Lett. **96**, 120602 (2006).
[42] M. A. Cuendet, J. Chem. Phys. **125**, 144109 (2006).
[43] E. Schöll-Paschinger and C. Dellago, J. Chem. Phys. **125**, 054105 (2006).
[44] B. L. Holian, G. Ciccotti, W. G. Hoover, B. Moran, and H. A. Posch, Phys. Rev. A **39**, 5414 (1989).
[45] Ji-Huan He, Phys. Rev. Lett. **90**, 174301 (2003); **91**, 199902(E) (2003).